Acta Materialia 57 (2009) pp. 3382-3390

Phase-field model study of the crystal morphological evolution of hcp metals

R.S. Qin[1*], H.K.D.H. Bhadeshia [1,2]

1. Graduate Institute of Ferrous Technology, Pohang University of Science and Technology, San 31, Hyojia-Dong Nam Gu, Pohang 790-784, Republic of Korea

2. Department of Materials Science and Metallurgy, University of Cambridge, Pembroke Street, Cambridge CB2 3QZ, United Kingdom

Abstract

An expression for anisotropic interfacial energy of hexagonal close-packed metals has been formulated which is able to reproduce published data obtained using the modified embedded atom method, covering the variation in interface energy as a function of orientation for a number of metals. It turns out that the coefficients associated with the expression can be determined fully by measured or calculated interfacial energies of just three independent crystal planes. Three-dimensional phase-field model simulations using this representation of interfacial energy have been found to yield convincing crystal morphologies. The apparent rate of crystal growth as a function of orientation in the phase-field simulation agrees with predictions made by surface energy theory.

Keywords: Phase-field modelling; Interfaces; Grain morphology; Anisotropy

*Corresponding author. Tel: +82 54 2794407; fax: +82 54 2794499.
Email address: rsqin@postech.ac.kr

1. Introduction

Interfacial energy (σ) and its orientation dependence is in a phase-field model expressed via a gradient energy coefficient ε [1-5], which scales with the square root of σ [6,7]. The calculation of the evolution of crystal morphology using phase fields requires a smooth analytical expression for ε as a function of orientation, because a second order differential of ε is required in the governing equation for the order parameter. There has been significant progress in the development of such expressions for cubic metals [1-5, 7]. Given a unit vector $\hat{n} = n_x\hat{x} + n_y\hat{y} + n_z\hat{z}$ representing the normal to an interface in orthonormal coordinates, the earliest approach supporting two-dimensional phase-field calculations was based on $\varepsilon = \bar{\varepsilon}\left[1 + \gamma_\varepsilon \cos\left(k_\varepsilon \theta\right)\right]$ [1], where $\bar{\varepsilon}$ is the mean value of ε, γ_ε and k_ε are anisotropy parameters, and $\theta = \arctan\left(n_y / n_x\right)$. For computations in three-dimensions, it was suggested at first that $\varepsilon = \bar{\varepsilon}\left[1 + \gamma_\varepsilon\left(n_x^4 + n_y^4 + n_z^4\right)\right]$ [4] but this has been modified into $\varepsilon = \bar{\varepsilon}\left[1 + \varepsilon_1 K_1\left(\theta,\phi\right) + \varepsilon_2 K_2\left(\theta,\phi\right) + \cdots\right]$ [5] after reviewing molecular dynamics simulations for dendrite growth which suggest that the addition of $\varepsilon_2 K_2(\theta, \phi)$ term gives a better representation of anisotropy, where $\theta = \arctan\left(\sqrt{n_x^2 + n_y^2} / n_z\right)$ and $\phi = \arctan\left(n_y / n_x\right)$ represent the orientation of the interface, ε_1 and ε_2 are coefficients reflecting the extents of anisotropy, $K_1(\theta, \phi)$ and $K_2(\theta, \phi)$ are cubic harmonics that are combinations of standard spherical harmonics with cubic symmetry. Recently, Qin and Bhadeshia suggested that the gradient energy coefficient can be expressed in the following format [7]

$$\varepsilon\left(\hat{n}\right) = \varepsilon_0 + \varepsilon_1\left(n_x^2 n_y^2 + n_y^2 n_z^2 + n_z^2 n_x^2\right) + \varepsilon_2 n_x^2 n_y^2 n_z^2 + \varepsilon_3\left(n_x^2 n_y^2 + n_y^2 n_z^2 + n_z^2 n_x^2\right)^2 \qquad (1)$$

where the associated coefficients can be determined by experimental measurement or numerical calculations such as those based on the embedded-atom method. This formula is proved to be able to describe published data obtained using the embedded atom method with good accuracy and to compute convincing crystal morphology.

The hexagonal close-packed (hcp) metals constitute a large proportion of metallic materials. However, there is no corresponding expression for the gradient energy coefficient in the context anisotropy. The development of this is the aim of the present work so as to enable the evolution of crystal morphology to be estimated using the phase field method.

2. Anisotropy of interfacial energy of hcp metals

The hcp crystal is conventionally represented as in Fig. 1(a), with the $[100]_h$ and $[010]_h$ axes subtending an angle of 120°. The $[001]_h$ axis is perpendicular to both $[100]_h$ and $[010]_h$. The ratio between vertical and horizontal cell-edges is denoted as *c/a*.

For the convenience of a phase-field description, the miller indices of planes in the hexagonal lattice are converted into a cubic coordinate system. There are two simple ways of doing this, as illustrated in Fig. 1(a) and 1(b), respectively. The conversion illustrated in Fig. 1(a) is defined by

$$\begin{pmatrix} h & k & l \end{pmatrix}_c = \begin{pmatrix} h & k & l \end{pmatrix}_h \begin{pmatrix} 1 & 1/\sqrt{3} & 0 \\ 0 & 2/\sqrt{3} & 0 \\ 0 & 0 & a/c \end{pmatrix} \tag{2}$$

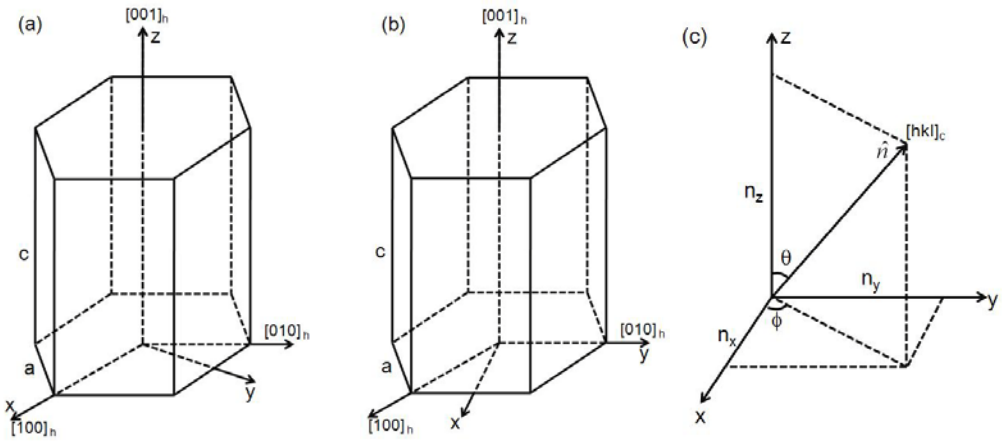

Fig. 1. Relation between hexagonal and cubic coordinates. (a). x-axis along the $[100]_h$ direction; (b) y-axis along the $[010]_h$ direction. (c) Relation between Miller indices, cubic and polar coordinates.

where the subscripts c and h represent the cubic and hexagonal coordinate systems respectively. The conversion for the case illustrated in Fig. 1(b) is given by

$$\begin{pmatrix} h & k & l \end{pmatrix}_c = \begin{pmatrix} h & k & l \end{pmatrix}_h \begin{pmatrix} 2/\sqrt{3} & 0 & 0 \\ 1/\sqrt{3} & 1 & 0 \\ 0 & 0 & a/c \end{pmatrix} \tag{3}$$

In cubic coordinates, as illustrated in Fig. 1(c), the normal to a plane with Miller indices $(hkl)_c$ plane is the direction $[hkl]_c$. The interface normal $\hat{n} = n_x\hat{x} + n_y\hat{y} + n_z\hat{z}$ can be represented in polar or spherical coordinates as follows:

$$n_x = \sin\theta\cos\phi = \frac{h_c}{\sqrt{h_c^2 + k_c^2 + l_c^2}} \tag{4.1}$$

$$n_y = \sin\theta\sin\phi = \frac{k_c}{\sqrt{h_c^2 + k_c^2 + l_c^2}} \tag{4.2}$$

$$n_z = \cos\theta = \frac{l_c}{\sqrt{h_c^2 + k_c^2 + l_c^2}} \tag{4.3}$$

where $\theta = \arctan\left(\frac{\sqrt{n_x^2 + n_y^2}}{n_z}\right) = \arctan\left(\frac{\sqrt{h_c^2 + k_c^2}}{l_c}\right)$ and $\phi = \arctan\left(\frac{n_y}{n_x}\right) = \arctan\left(\frac{k_c}{l_c}\right)$.

The expression for the anisotropy of interfacial energy could contain a factor of $n_x^6 - 6n_x^4 n_y^2 + 9n_x^2 n_y^4$ in order to generate the required hexagonal geometry, and also a factor of n_z^m where *m* must be an even number to be consistent with the symmetry along the $[001]_h$ direction. The simplest resulting expression is therefore $\sigma(\hat{n}) = k_0 + k_1 n_z^m + k_2\left(n_x^6 - 6n_x^4 n_y^2 + 9n_x^2 n_y^4\right)$.

To validate the expression and determine the value of *m*, the proposed $\sigma(\hat{n})$ was fitted to published interfacial energy data calculated using the modified embedded-atom method (MEAM) [8,9], which when compared with the original embedded atom method (EAM) [10,11], includes the directional bonding of the atoms in crystals [12-14]. The parameters in the interatomic potentials that are used in the MEAM computation of interface energy of hcp metals were developed by Baskes and Johnson [13]. Zhang *et al.* and Wang *et al.* reported the surface energies of 34 planes [8,9]. Some of the planes have two values available corresponding to two possible termination mechanisms in hcp lattices. The smaller of the two should be preferred in the determination of the crystal shape according to Wulff's theorem [15]; therefore, only the smaller value was considered in the analysis presented here.

The data fitting was achieved using the least squares method, for which the objective function is defined as

$$\delta = \sum_i \left[\sigma(\hat{n}) - \sigma_{MEAM}(\hat{n})\right]^2 \tag{5}$$

where i equals the number of available MEAM data (34 in the current work), $\sigma(\hat{n})$ is the proposed expression and $\sigma_{MEAM}(\hat{n})$ from MEAM data. The best values of k_0, k_1, and k_2 are obtained when δ achieves a minimum, *i.e.,* at $\partial\delta / \partial k_j = 0$ with j=*0, 1,* and *2*. The deviation between $\sigma(\hat{n})$ and the $\sigma_{MEAM}(\hat{n})$ is represented by the average relative error (AvRE), defined as $AvRE = \overline{\left[\left|\sigma(\hat{n}) - \sigma_{MEAM}(\hat{n})\right| / \sigma_{MEAM}(\hat{n})\right]}$ where the bar means average, and the averaging procedure goes through all available orientations of the interface energy.

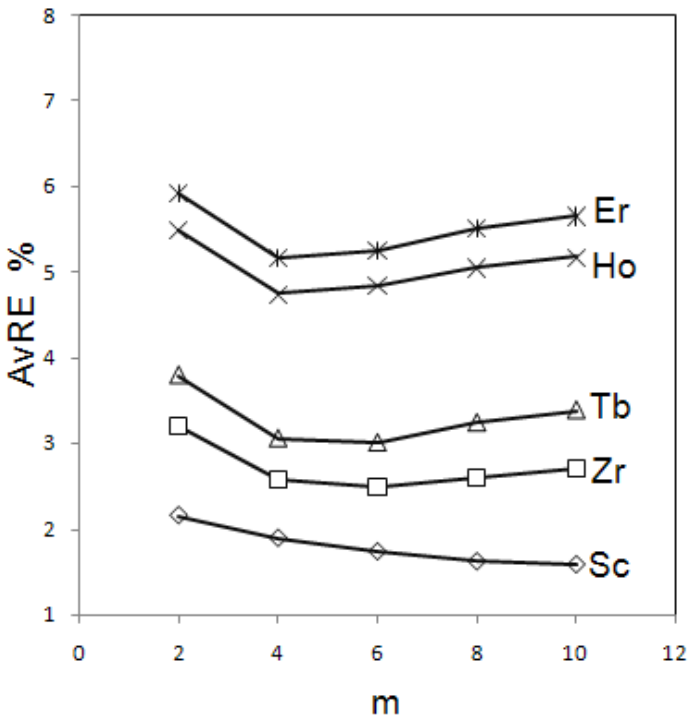

Fig. 2. Comparison of the accuracy between numerical results from MEAM and values by $\sigma(\hat{n}) = k_0 + k_1 n_z^m + k_2\left(n_x^6 - 6n_x^4 n_y^2 + 9n_x^2 n_y^4\right)$ as a function of the exponent m of n_z.

The first step is to assess the value of *m*. For this purpose we tried *m = 2, 4, 6, 8*, and *10*. The results are demonstrated in Fig. 2. It can be seen from Fig. 2 that *m = 6* gives the best accuracy for majority of materials, although other values of *m* might provide less AvRE numbers for a few individual materials. It is therefore applied *m=6* in following calculations and defines

$$\sigma(\hat{n}) = k_0 + k_1 n_z^6 + k_2\left(n_x^6 - 6n_x^4 n_y^2 + 9n_x^2 n_y^4\right) \tag{6}$$

To compare the interface energies calculated using Eq. (6) with the MEAM data reported in reference [8], Eq. (3) was used to express the Miller indices in the cubic coordinates illustrated in Fig 1(b). The corresponding anisotropy coefficients and the average relative errors for 13 metals are listed in Table 1. Eq. (6) contains only three unknown coefficients, which means that they can in principle be determined using the interfacial energies from just three independent planes. To prove this, the coefficients were estimated using only the surface energies for $(100)_h$, $(110)_h$ and $(001)_h$; the results are in Table 1 (column entitled AvRE3). It is evident that using information from just three planes to fix the coefficients in equation (6) gives a satisfactory description for all the planes of hcp metals.

Table 1 Anisotropy coefficients k_0, k_1, k_2 and AvRE determined by least squares fitting of MEAM data. The units for coefficients are in erg/cm^2. AvRE3% is for the data plotted in Fig. 4.

Metal	k_0 (erg/cm^2)	k_1 (erg/cm^2)	k_2 (erg/cm^2)	AvRE (%)	AvRE3 (%)
Co	4849.39	-2001.72	-931.167	5.57	5.57
Dy	2780.3	-782.961	-179.021	5.95	5.20
Er	2777.18	-751.604	-205.811	5.25	4.86

Gd	1481.82	-241.978	-106.965	2.19	3.15
Ho	2487.53	-579.579	-131.261	4.84	4.59
Mg	1425.55	-574.717	-244.316	6.14	5.74
Nd	2477.12	-888.073	-408.88	4.58	4.79
Pr	1965.19	-625.91	-293.58	3.61	4.07
Re	4423.69	-601.51	-249.68	1.90	3.21
Sc	1403.67	-114.551	-52.5072	1.73	3.38
Tb	1790.92	-391.351	-161.747	3.01	3.54
Tl	1131.91	-466.913	-213.432	5.74	5.76
Zr	2709.42	-441.208	-144.752	2.49	3.42

Wang *et al.* provided MEAM interfacial energy data for Be, Hf, Ru, Ti and Y [9]. Eq. (2) was applied to express the plane indices in cubic coordinates. The associated anisotropy coefficients and the average relative errors for those 5 metals are presented in table 2. The AvRE numbers calculated by Eq. (6) with coefficients determined by $(100)_h$, $(110)_h$ and $(001)_h$ planes are listed in table 2 with column entitled AvRE3.

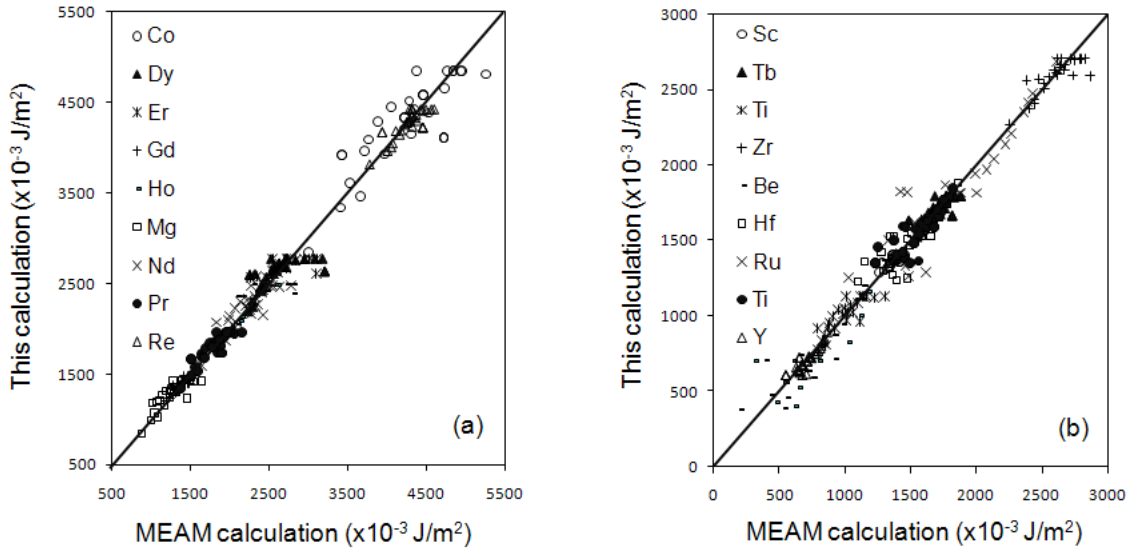

Fig. 3. Comparison of interface energy calculated by Eq. (6) where anisotropy coefficients are determined by Eq. (6) using MEAM data.

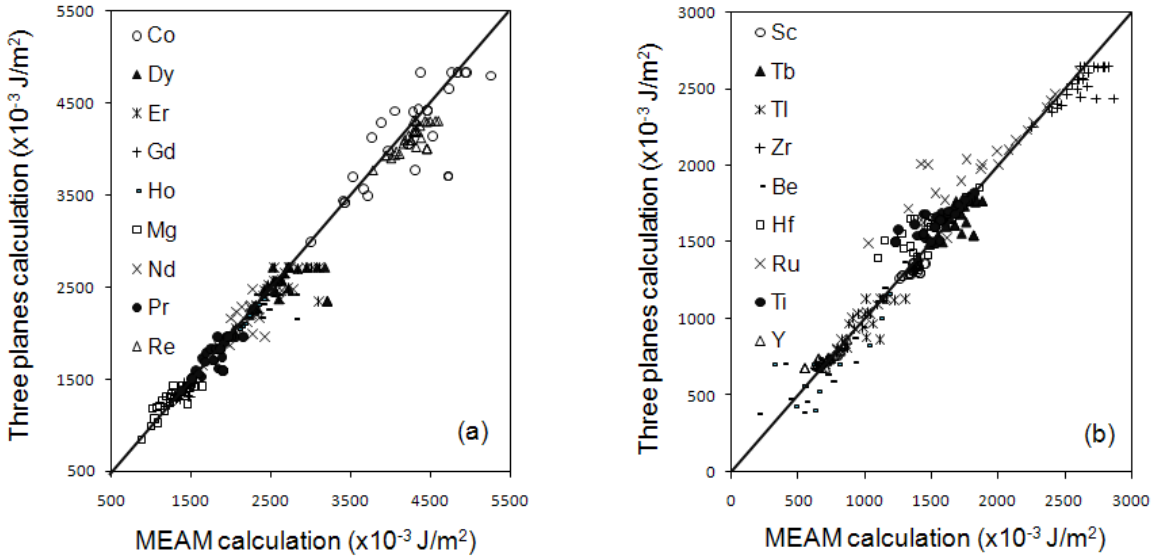

Fig. 4. Comparison of interface energy calculated by Eq. (6) where anisotropy coefficients are determined interface energies at $(100)_h$, $(110)_h$ and $(001)_h$ planes using MEAM data.

The calculations for Be are not satisfactory. An examination of the original MEAM data [9] shows that the interface energy for $(001)_h$ plane is 1285.9 ergs/cm^2 but only 197.7 ergs/cm^2 in $(110)_h$. The latter is less than 1/6 of the energy for the basal plane and is much less than the energies of semi-coherent interfaces [16]. The abnormal interfacial energy value for $(110)_h$ plane for Be leads to further discrepancies when the coefficients are determined using only the $(100)_h$, $(110)_h$ and $(001)_h$. The AvRE values for Hf, Ti and Y are acceptable. Fig. 3 illustrates the comparison of all MEAM calculations with the Eq. (6) where the anisotropy coefficients k_0, k_1 and k_2 are determined by the least squares method. Fig. 4 shows the case where the anisotropy coefficients in the Eq. (6) were determined using information from just the $(100)_h$, $(110)_h$, and $(001)_h$ planes. The comparison between the proposed expression of surface energy, Eq. (6), and the original MEAM data that were used

to determined the parameters of the expression for Co, Gd, Nd, Pr, Hf and Ti metals are demonstrated in Fig. 5, where the rainbow-coloured surface represents the numerical values by Eq. (6) and purple balls represent the MEAM data. The shadowed balls mean that they are inside the surface. A ball is inside, outside or embedded on the surface represents that the MEAM values are smaller, larger or about the same as the value by proposed expression. The closer a ball to the surface implies the better fitting. The rainbow colour of the surface represents the smooth changing of surface energy from its largest (represented by red colour) to its smallest (represented by blue colour).

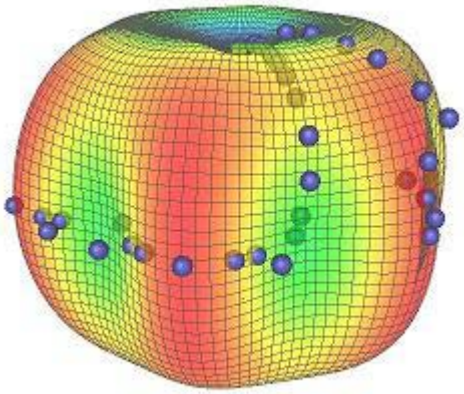

Co

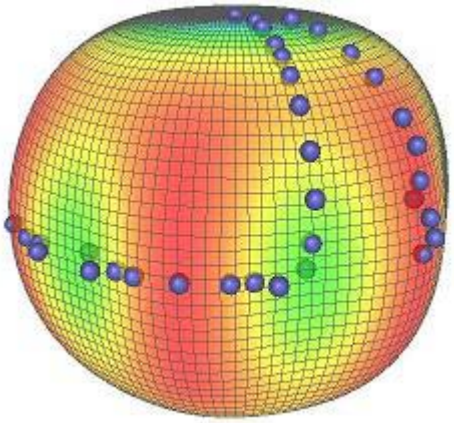

Gd

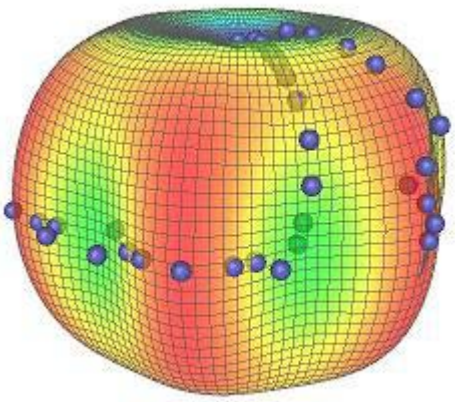

Nd

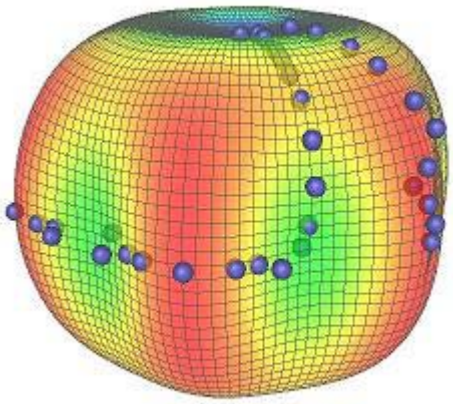

Pr

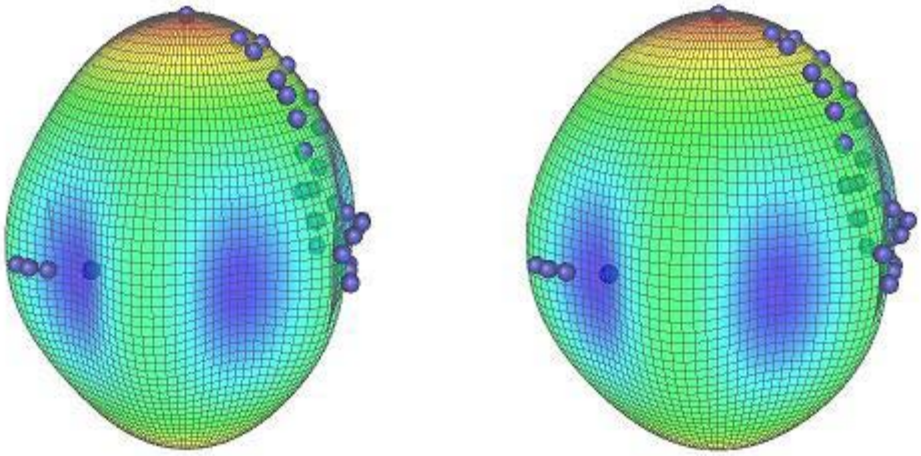

Hf Ti

Fig. 5. Comparison of interface energy calculated by Eq. (6) with the original MEAM data for Co, Gd, Nd, Pr, Hf and Ti. The numerical values from Eq. (6) are represented by rainbow-coloured surface (colour changes from red to blue represents the surface energy goes from its largest value to the smallest). MEAM data are represented by purple balls. The shadow balls implies they are located inside the surface. The closer a ball to the surface implies the better fitting.

Table 2 Anisotropy coefficients k_0, k_1, k_2 and AvRE determined by least squares fitting of MEAM data. The units for coefficients are in erg/cm^2. AvRE3% is for the data plotted in Fig. 4.

Metal	k_0	k_1	k_2	AvRE (%)	AvRE3(%)
Be	701.986	665.446	-319.98	24.24	34.08
Hf	1529.39	353.494	-297.401	5.2865	8.988
Ru	1815.37	872.827	-564.817	7.411	12.58
Ti	1590.69	261.408	-244.217	4.414	7.149
Y	723.886	168.206	-115.635	3.6478	5.77

The basic difference between anisotropy coefficients listed in tables 1 and 2 is the sign of k_1. In table 2, $k_1>0$ reflects the fact that $(001)_h$ plane has the maximum surface energy, and vice versa for $k_1<0$ in table 1. Fig. 6 shows the interfacial energies of Y and Tb from different perspectives.

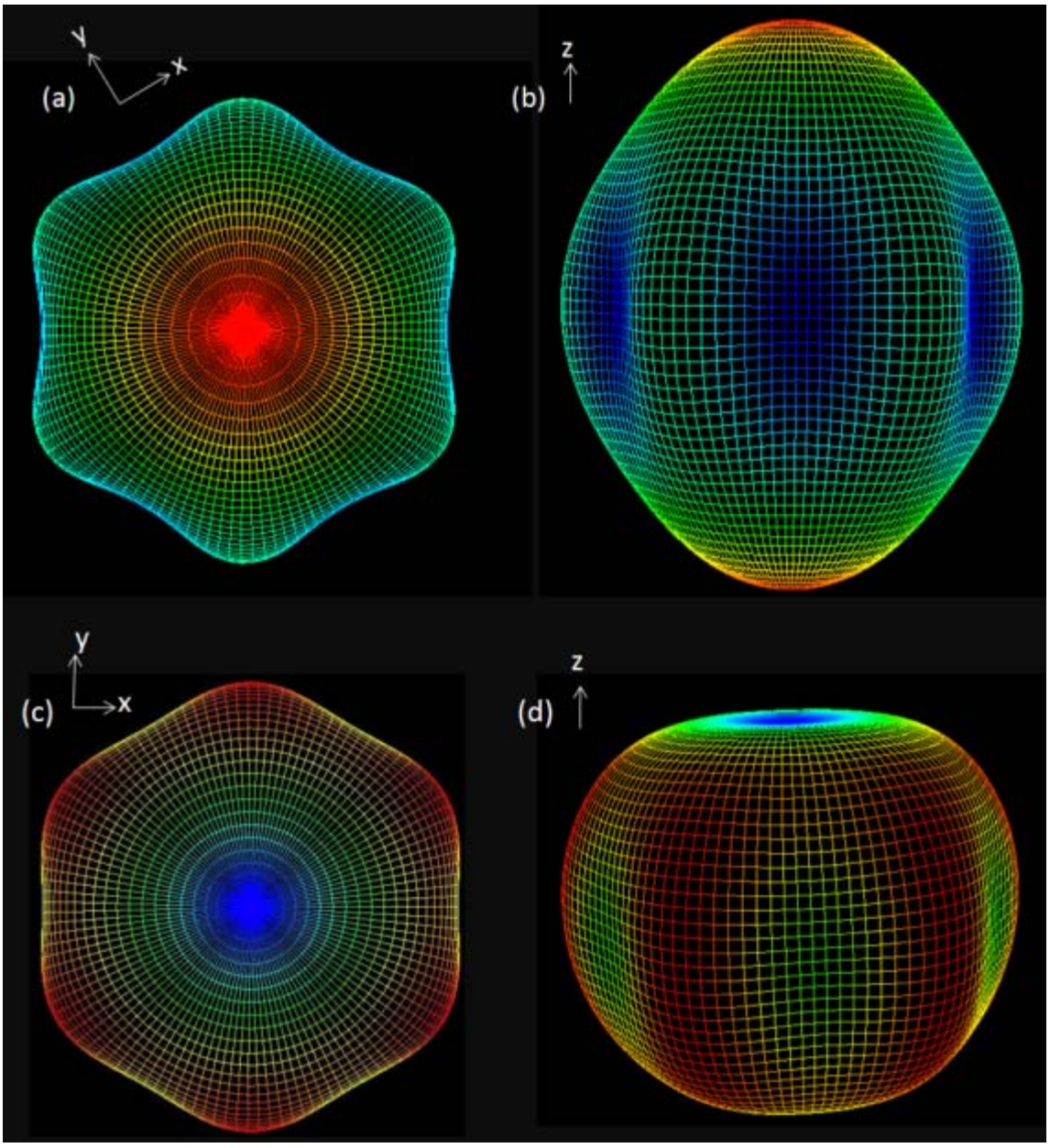

Fig. 6. Anisotropy of interfacial energy (red is the highest and blue the lowest energy). (a) and (b) Y; (c) and (d) Tb.

3. Gradient energy coefficients and phase-field model

Cahn-Hoffman ξ vector theory is used to describe the interface anisotropy in a phase field model [17,18]. n_x, n_y and n_z in Eq. (6) are replaced by $\frac{1}{|\nabla\varphi|}\frac{\partial\varphi}{\partial x}$, $\frac{1}{|\nabla\varphi|}\frac{\partial\varphi}{\partial y}$ and $\frac{1}{|\nabla\varphi|}\frac{\partial\varphi}{\partial z}$, respectively, where φ is the phase-field order parameter which is introduced to represent the physical state of the material at any location. $\varphi = 0$ and $\varphi = 1$ represent two bulk phases and $0<\varphi<1$ represents interface. For convenience the free energy density of the system is defined as [6,7]

$$g(\varphi) = \frac{1}{2}\varepsilon^2|\nabla\varphi|^2 + \frac{1}{4\omega}\varphi^2(1-\varphi)^2 + g_b(\varphi) \tag{7}$$

where ω is a coefficient reflecting the kinetic barrier between two minima in the double-well potential representation. $g_b(\varphi) = [1-h(\varphi)]g_0 + h(\varphi)g_1$, $h(\varphi) = \varphi^3(6\varphi^2 - 15\varphi + 10)$, g_0 and g_1 are free energy densities of bulk phases with $\varphi=0$ and $\varphi=1$, respectively. In all reported work on the simulation of cubic metals, the gradient energy coefficient ε is represented as a polynomial expansion of n_x, n_y and n_z. The present work suggests a different approach, as follows.

In our previous work the relation between gradient energy coefficient $\varepsilon(\hat{n})$ and interface energy $\sigma(\hat{n})$ in direction $\hat{n}$ was shown to satisfy [7]

$$\sigma(\hat{n}) = \frac{1.1}{3\lambda}\varepsilon(\hat{n})^2 \tag{8}$$

where λ is the half-thickness of the interface. Representing $\varepsilon(\hat{n})$ as

$$\varepsilon(\hat{n}) = \varepsilon_0 \eta(\hat{n}) \tag{9}$$

Eq. (9) is similar to an early suggestion for the gradient energy coefficient in two-dimensional phase-field simulation of cubic metals [1]. On combining Eqs (6) and Eq. (8) and comparing with Eq. (9), it is seen that

$$\varepsilon_0 = \sqrt{3\lambda k_0 / 1.1} \tag{10}$$

$$\eta(\hat{n}) = \sqrt{1 + \frac{k_1}{k_0} n_z^6 + \frac{k_2}{k_0}\left(n_x^6 - 6n_x^4 n_y^2 + 9n_x^2 n_y^4\right)} \tag{11}$$

ε_0 does not have the meaning of average value of gradient energy coefficient. This is different from the original definition in other earlier work. The format of $\eta(\hat{n})$ is completely unfamiliar, but its computation does not appear to present particular difficulties.

The governing equation for the evolution of phase-field order parameter takes the following format

$$\frac{\partial \varphi}{\partial t} = M_\varphi \left\{ \varepsilon_0^2 \frac{\partial}{\partial x}\left[|\nabla \varphi|^2 \eta(\hat{n}) \frac{\partial \eta(\hat{n})}{\partial(\varphi_x)} \right] + \varepsilon_0^2 \frac{\partial}{\partial y}\left[|\nabla \varphi|^2 \eta(\hat{n}) \frac{\partial \eta(\hat{n})}{\partial(\varphi_y)} \right] + \frac{\partial}{\partial z}\left[\varepsilon_0^2 |\nabla \varphi|^2 \eta(\hat{n}) \frac{\partial \eta(\hat{n})}{\partial(\varphi_z)} \right] \right.$$

$$\left. + \varepsilon_0^2 \nabla\left[\eta(\hat{n})^2 \nabla \varphi\right] - \frac{1}{2\omega}\varphi(1-\varphi)(1-2\varphi) - 30\varphi^2(1-\varphi)^2(g_0 - g_1) \right\} \tag{12}$$

4. Numerical computation and discussion

Based on the MEAM data for the interfacial energies of hcp metals presented in section 2, it is appropriate to categorize the hcp metal into two groups. The first group possesses the largest interface energy at $(001)_h$ plane and with $k_1>0$. The second group has $k_1<0$ and the

interface energy at $(001)_h$ plane is not the largest. It is known from experiments that the morphology of crystal in basal plane should be topological hexagon to reflect the nature of hcp lattice. It is also expected that the crystal will grow at the greatest rate along the direction with the largest interface energy so as to reduce the total surface energy for a given volume. For example, if $(001)_h$ possesses the largest interface energy, the crystal should elongate along the $[001]_h$ direction and finally leave the smallest surface area parallel to $(001)_h$. Wulff's theorem can be used to predict the equilibrium crystal shape. For non-equilibrium crystal growth, although the shape is not necessarily consistent with equilibrium, it is feasible that the growth morphology is dominated by the equilibrium shape especially when the driving force for growth is not excessive.

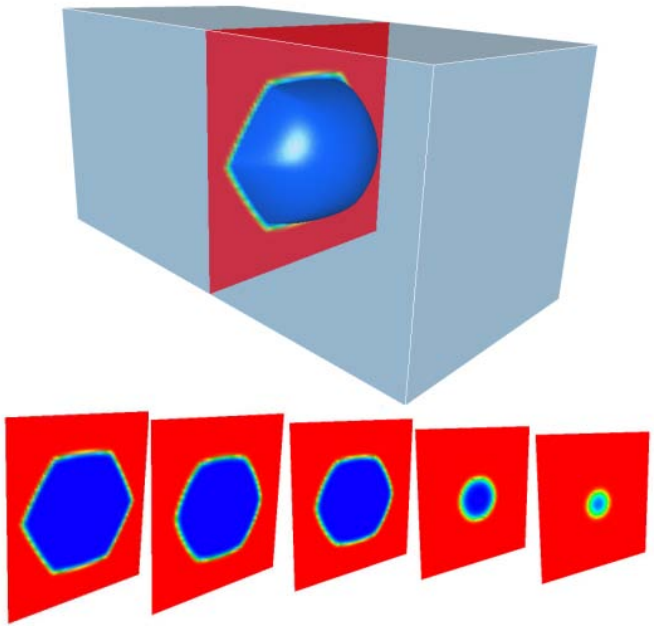

Fig. 7. Crystal morphology at 12000 time steps with anisotropy parameters k_0 =1.8 J/m^2, k_1 =0.6 J/m^2 and k_2 = - 0.1 J/m^2. The sections from left to right are along z = 94, 106, 152, 172 and 178 grid position. The blue colour corresponds to φ=1, red colour φ=0 and rainbow $0<\varphi<1$.

With this in mind, three types of phase-field simulations have been carried out. The first is with anisotropy coefficients chosen arbitrarily. The second and third cases utilise the anisotropy coefficients of Y and Tb respectively. The parameters are listed in table 3.

Table 3 Anisotropy coefficients applied in phase-field computations of Figs. 7-9.

	k_0 (J/m^2)	k_1 (J/m^2)	k_2 (J/m^2)
Case 1	1.8	0.6	-0.1
Case 2	0.723886	0. 168206	-0.115635
Case 3	1.79092	-0.391351	-0.161747

Other parameters in phase-field simulations are identical for all three cases with $g_0 - g_1 = 3.68596 \times 10^8$ J/m^3, $M_\varphi = 100$ and $\lambda = 14.3$ nm [19, 20] in the simulations. ω is determined by $\omega = \lambda^2 / \left(2.42\varepsilon_0^2\right)$ [6]. Eq. (12) is solved by a 6-neighbour implicit finite difference method on three-dimensional grids. The grid size is chosen as $\Delta x = 0.5\lambda$ so that interface covers 4 elements [20, 22]. The initial condition is to put a spherical seed at the centre of the logistic frame with the phase-field order parameter configured to

$$\begin{cases} \varphi(r, t=0) = 1 & for \quad r < \Delta x \\ \varphi(r, t=0) = \dfrac{2}{1+\exp(r-1)} & for \quad \Delta x < r < 4\Delta x \\ \varphi(r, t=0) = 0 & for \quad r \geq 4\Delta x \end{cases} \tag{13}$$

The system with case 1 parameters listed in table 3 is computed in 90×90×200 grids. The crystal shape at 12000 time steps is illustrated in Fig. 7, together with slices at z = 94, 106, 152, 172 and 178. The colours from dark to light (blue to red) correspond to φ from 1 to 0.

It is obvious that the crystal morphology of the basal plane is consistent with hexagonal symmetry.

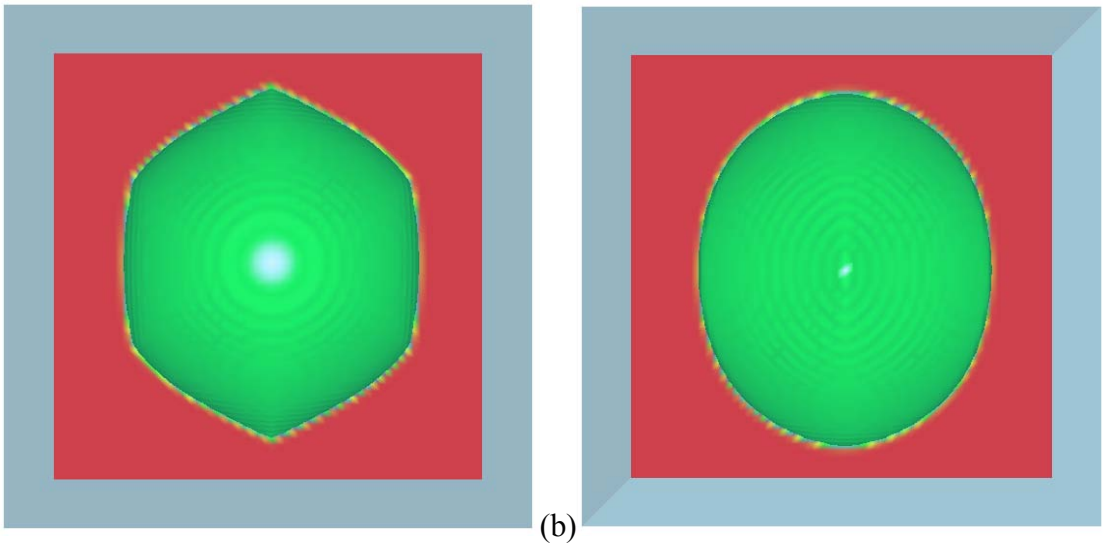

(a) (b)

Fig. 8. Crystal shape at 20000 time steps with the anisotropy parameters k_0 =0.723886 J/m^2, k_1 = 0. 168206 J/m^2 and k_2 = -0.115635 J/m^2, where the green colour represents φ=0.5 (growing crystal interface), red colour φ=0 (original matrix) and outside frame is for three dimension visualization effect. (a) View along $[001]_c$. (b) Viewing along $[100]_c$.

Fig. 8 illustrates the crystal morphology at 20000 time steps using the anisotropic parameters of Y at 128×128×128 grids. The green colour represents φ=0.5 (growing crystal interface), red colour φ=0 (original matrix) and outside frame is for three dimension visualization effect. Fig. 8(a) is viewed along $[001]_c$ towards the centre of the crystal and demonstrates the hexagonal symmetry. Fig. 8(b) is viewed from a position perpendicular to $[001]_c$ axis and with $[001]_c$ in vertical, which shows that the crystal grows faster along $[001]_c$ direction then other directions. When k_1 >0 the crystal elongates along $[001]_c$ to minimise the surface area on $(001)_c$. This agrees with the prediction described earlier.

Fig. 9 illustrates the crystal morphology at 17000 time steps for the same grid as Fig. 8 using the parameters for Tb. The colours have the same meaning as that of in Fig. 8. The view along $[001]_c$ is again consistent with the hexagonal symmetry, and Fig. 9(b) shows that the crystal grows slowest along $[001]_c$, which is along the vertical direction. This is due to the fact of $k_1 < 0$ which implies that the interface energy at $(001)_c$ plane is smaller. In this case the crystal grows faster normal to maximise the area of the low—energy plane $(001)_c$.

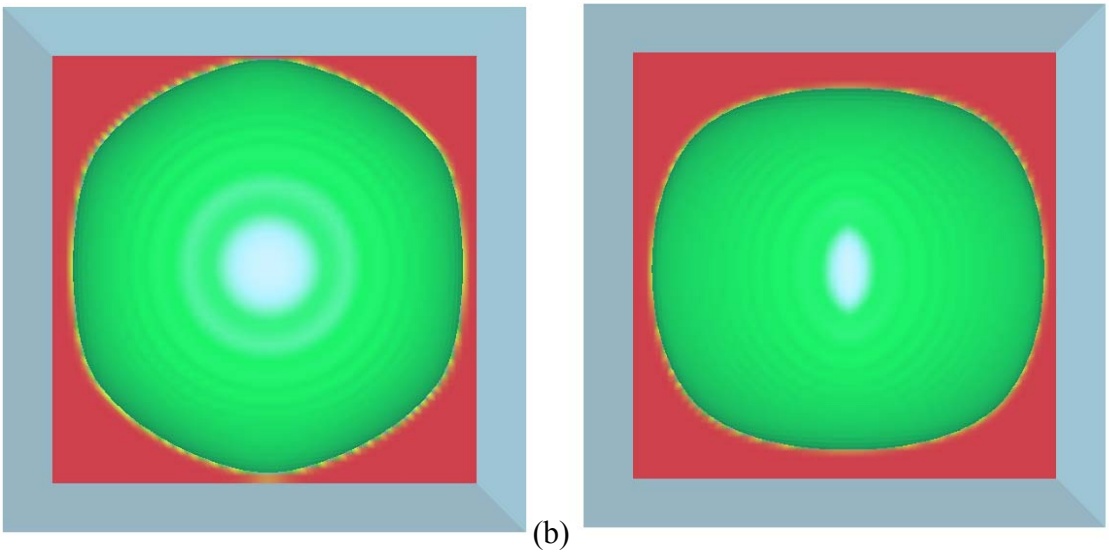

(a) (b)

Fig. 9. Crystal shape at 17000 time steps with the anisotropy parameters k_0 =1.79092 J/m^2, k_1 = -0.391351 J/m^2 and k_2 = -0.161747 J/m^2. The colours have the same meaning as that of in Fig. 8. (a) Viewing along $[001]_c$. (b) Viewing along $[100]_c$.

5. Conclusions

(1) An expression for the anisotropic interface energy of hcp metals is suggested to be $\sigma(\hat{n}) = k_0 + k_1 n_z^m + k_2\left(n_x^6 - 6n_x^4 n_y^2 + 9n_x^2 n_y^4\right)$ with *m* an even number, taken here to be 6 in order to account for published data on the orientation dependence of interfacial energy in hexagonal close-packed metals.

(2) The coefficients k_0, k_1 and k_2 have been determined by comparison with published data calculated using the embedded-atom method. Our analysis reveals that since it is sufficient to consider just three interfaces to solved for the coefficients, future attempts at calculating interfacial energies need not explore a large set of interface orientations in order to define the anisotropy. Indeed, it has been demonstrated that the published data can essentially be explained by deriving the coefficients from the data for just $(100)_h$, $(110)_h$ and $(001)_h$.

(3) The gradient energy coefficient in phase-field model can be represented as $\varepsilon(\hat{n}) = \varepsilon_0 \eta(\hat{n})$, where $\varepsilon_0 = \sqrt{3\lambda k_0 / 1.1}$ and $\eta(\hat{n}) = \sqrt{1 + \frac{k_1}{k_0} n_z^6 + \frac{k_2}{k_0}\left(n_x^6 - 6n_x^4 n_y^2 + 9n_x^2 n_y^4\right)}$.

(4) Phase-field simulations demonstrate convincing hcp crystal morphologies, consistent with evolution towards an equilibrium shape calculated on the basis of interfacial energy minimisation.

Acknowledgements

The authors are grateful to Professor Hae-Geon Lee for the provision of laboratory facilities at the Graduate Institute for Ferrous Technology, POSTECH.

References

[1] Wheeler AA, Murray BT. Physica D 1993;66:243.

[2] Karma A, Rappel WJ. Phys Rev E 1998; 57:4323.

[3] Haxhimali T, Karma A, Gonzales F, Rappaz M. Nature Mater. 2006; 5:660.

[4] Moelans N, Blanpain B, Wollants P. Phys Rev Lett 2008; 101:025502.

[5] Loginova I, Ågren J, Amberg G. Acta Mater. 2004; 52:4055.

[6] Kim SG, Kim WT, Suzuki T. Phys Rev E 1998; 58:3316.

[7] Qin RS, Bhadeshia HKDH. Acta Mater. 2009; 57:2210.

[8] Zhang JM, Wang DD, Xu KW. Appl Surf Sci. 2006; 253:2018.

[9] Wang DD, Zhang JM, Xu KW. Surf Sci. 2006; 600:2990.

[10] Prieto JE, Muller CRS, Miranda R, Heinz K. Surf Sci. 1998; 401:248.

[11] Zhang JM, Xu KW. Prog. Cryst. Growth Char Mater. 2000:40:315.

[12] Zhang JM, Xu KW. Appl Surf Sci. 2003; 218:245.

[13] Baskes MI, Johnson RA. Modell Simul Mater Sci Eng 1994:2:147.

[14] Rose JH, Smith JR, Guinea F, Ferrante J. Phys Rev B 1984; 29:2963.

[15] Wulff G. Z Kristallogr 1901;34:449.

[16] Johansson SAE, Christensen M, Wahnström G, Phy Rev Lett 2005:95:226108.

[17] Wheeler AA, McFadden GB. Proc R Soc London A 1997;453:1611.

[18] Nestler B, Wheeler AA. Phys Rev E 1998; 57:2602.

[19] Qin RS, Wallach ER. Acta Mater. 2003; 51:6199.

[20] Warren JA, Boettinger WJ. Acta Metall Mater. 1995;43:689.